FirePhysChem 3 (2023) 121–127

Contents lists available at ScienceDirect

FirePhysChem

journal homepage: http://www.keaipublishing.com/cn/journals/firephyschem/

Purification, crystal structure and properties of azoxytriazolone (AZTO)

Tianlong Zhou[a], Jiaxu Gong[a], Mingzhen Xie[a], Bozhou Wang[b], Yifan Jiang[b], Jiaheng Wang[a], Jie Zhou[a], Linzhi Zhong[a], Yatang Dai[a,*]

[a] State Key Laboratory of Environment-Friendly Energy Material, School of Materials Science and Engineering, Southwest University of Science and Technology, Mianyang 621010, PR China
[b] Xi'an Modern Chemistry Research Institute, Xi'an 710069, PR China

ARTICLE INFO

Keywords:
Azoxytriazolone
Separation and purification
Thermal stability
Crystal structure
Sensitivity

ABSTRACT

In this work, the azoxytriazolone (AZTO) was synthesized by electrochemical reduction 5-nitro-1,2,4-triazol-3-one (NTO) under different types of electrolytes which were Na_2SO_4 and H_2SO_4. By comparing the yield of AZTO/azoTO synthesized under different electrolyte conditions, the work found that sulfuric acid as the electrolyte has a positive effect on the synthesis of AZTO. On this basis, the high-concentration AZTO was prepared by regulating the concentrations of sulfuric acid (0.05M, 0.1M, 0.5M, 1M). Finally, by introducing an appropriate amount of NaOH, we successfully achieved the separation and purification of AZTO from the mixture of AZTO and azoTO. In addition, single crystal AZTO was also prepared in this experiment to test its crystal structure, which illustrated that the crystal density of AZTO is 1.902 g/cm^3 at 193 K, belonging to the monoclinic crystal system with space group $P2_1/n$. The thermal properties results of AZTO showed that the thermal stability properties of AZTO were affected by AZTO/azoTO ratio, and the thermal decomposition peak of pure AZTO is 352°C when the content of azoTO is zero. On the contrary, the BAM susceptibility tester test demonstrated the impact susceptibility is 30 J and the friction susceptibility is greater than 360 N of AZTO, which are unaffected on azoTO. According to the K-J empirical formula, the blasting velocity and detonation pressure of AZTO were 7713.5 m/s and 26.1 GPa, respectively. The influences of different types of electrolytes and sulfuric acid concentrations on the yield of AZTO were evaluated, and the relevant reaction mechanism of electrochemical synthesis of AZTO and azoTO was supplemented in this paper.

1. Introduction

With the continuous expansion of the application scope of energetic materials, more and more attention has been paid to the environmental impact of the synthesis and application of energetic materials. At the same time, more and more research has also focused on the development of green synthetic methods and treatment of manufacturing waste, as well as the design and synthesis of safer and more environmentally friendly energy materials [1–6]. Among many compounds, nitrogen-rich compounds have high-energy N-N and C-N bonds, and their decomposition products are mainly friendly N_2, which is environmentally friendly. Therefore, it is an ideal energetic material. Compared with traditional energetic materials, high nitrogen compounds have the characteristics of high formation enthalpy and good stability, and the carbon monoxide and dust produced during combustion are less than other organic explosives due to their higher nitrogen content {[7] #66; [8] #68}. However, the synthesis of these high-nitrogen compounds is facing unprecedented challenges. In the synthesis of high nitrogen compounds, strong oxidants or reducing agents such as potassium permanganate, hydrazine hydrate, and hydrogen peroxide are needed {[9] #70; [10] #71}. And for some heterocyclic energetic materials containing nitrogen, their synthesis sometimes requires the use of toxic or heavy metal catalysts {[11] #75}. In view of this, an electrochemical synthesis method is proposed to solve these problems. Electrochemical synthesis refers to the use of electrons as oxidants or reducing agents without additional oxidant or reducing agents for reaction without adding other additives, which decreases the cost of materials synthesis and waste treatment, and reduces the difficulty of product separation and purification. The method has mild reaction conditions and does not require additional heating equipment {[12] #76; [13] #77; [14] #78}. A number of related studies have been reported, for example, Longrui Chen et al. constructed a flow device to achieve the synthesis of 100 g quantities of cyclobutane by electrochemical oxidation {[15] #49}; Huichao He et al. designed and synthesised W and Mo co-doped $BiVO_4$ thin film electrodes and synthesised azotetrazoles by electrochemical methods of oxidative dehydrogenation coupling under room temperature light conditions {[16] #79}; wastewater treatment by electrochemical methods was also subjected to great interest. NTO (5-nitro-1,2,4-triazol-3-one) is a blunt high-energy den-

* Corresponding author.
E-mail address: daiyatang@swust.edu.cn (Y. Dai).

https://doi.org/10.1016/j.fpc.2022.12.002
Received 31 October 2022; Received in revised form 13 December 2022; Accepted 15 December 2022
Available online 16 December 2022
2667-1344/© 2022 Xi'an Modern Chemistry Research Institute. Publishing services by Elsevier B.V. on behalf of KeAi Communications Co. Ltd. This is an open access article under the CC BY-NC-ND license (http://creativecommons.org/licenses/by-nc-nd/4.0/)

sity compound that is difficult to treat by conventional methods such as adsorption carbon scrubbers due to its high water solubility (1.28 g/100 mL at 19 °C) {[17] #80; [18] #81}. Wallace et al. proposed affordable remediation of wastewater by electrochemical methods, requiring only electrical input, no other additional chemical loading, and giving access to the insensitive energetic compound azoxytriazolone (AZTO) of some value, which can be obtained by direct filtration with low recovery costs due to the low solubility of AZTO in water {[19] #82}. However, AZTO is highly susceptible to further reduction to azotriazolone (azoTO) and the relatively similar nature of the two makes it difficult to purify by column chromatography and recrystallisation, thus making it impossible to obtain pure AZTO, which limits its further application {[20] #83}.

In this work, the influence of electrolyte type on the synthesis of AZTO and azoTO was studied and obtained better reaction conditions for the preparation of high-yield AZTO by optimizing the electrolyte concentration. Then, AZTO and azoTO were separated and purified for the first time by salt formation reaction. Moreover, the purity, crystal structure, thermal stability, and mechanical sensitivity properties of AZTO prepared from this experiment were analyzed and compared by single crystal X-ray diffraction, infrared spectroscopy, nuclear magnetic resonance hydrogen spectroscopy, comprehensive thermal analysis (TGA-DSC), and elemental analysis. Finally, the detonation performance was predicted by K-J empirical formula.

2. Experiment section

2.1. Material and methods

General: Unless otherwise stated, all reagents and solvents were used as is(Aladdin). Thermogravimetric (TG) and differential scanning calorimetry (DSC) tests were carried out using the SDT Q160 produced by the TA instrument in the nitrogen atmosphere with a heating rate of 10 K/min in an alumina disc. ^{1}HNMR spectra were measured by the JEOLGSX-600, and all samples used for NMR hydrogen spectroscopy were dissolved in dimethyl sulfoxide (DMSO-d_6). Chemical shifts were expressed in ppm relative to TMS(1H) and all samples used for NMR hydrogen spectroscopy were dissolved in dimethyl sulfoxide (DMSO-d_6). The infrared spectra of the samples in the range of 400-4000 cm^{-1} were recorded by the KBr tableting method using Nicolet 5700 Fourier transform infrared spectrometer (FT-IR). Elemental analysis(C, H, and N) was determined by the Vario EL CUBE-Elemental Analyzer. The crystal structure of AZTO was determined by single crystal X-ray diffraction. The data collection was performed on a Bruker APEX-II CCD X-ray diffractometer (Bruker Germany) with highly oriented graphite crystal monochromated GaK/α radiation (λ = 0.71073). The crystal was kept at 193K during data collection. Using Olex2 {[21] #85}, the structure was solved with the SHELXT {[22] #86} structure solution program using Intrinsic Phasing and refined with the SHELXL {[23] #87} refinement package using Least Squares minimisation. In this paper, all Cyclic Voltammetry (CV) tests and electrolysis experiments were performed in the CHI 760 electrochemical workstation (Shanghai, China). 3-Nitro-1,2,4-triazol-5-one (NTO) was synthesized according to the method reported in the literature {[24] #84}.

2.2. Syntheses of azoxytriazolone(AZTO)

The compound of AZTO was prepared according to the method reported by Wallace et al. {[25] #45}. 500 mg NTO was dissolved in 50 ml 0.1 mol/L H_2SO_4 aqueous solutions. In a single electrolysis chamber, a carbon working electrode, platinum counter electrode, and Ag/AgCl reference electrode were used for electrolysis at -1 V and 5 °C for 8 h. Then the mixture of AZTO and azoTO was obtained by filtration, and an appropriate amount of NaOH aqueous solution was added until AZTO was completely dissolved in water. The remaining azoTO was obtained by filtration drying with a yield of 10.2%. Subsequently, concentrated sulfuric acid was used to acidify the filtrate to produce a large amount of yellow-green precipitate. AZTO was obtained by filtration and drying, and the yield was 51.2%.

Azoxytriazolone (AZTO) ^{1}HNMR (600MHz, DMSO-d_6, ppm) δ = 13.20 (s, 1H), 12.48 (s, 1H), 12.45 (s, 1H), 12.08 (s, 1H). ^{13}C NMR (150Mz, DMSO-d_6, ppm) δ = 144.85, 146.40, 154.10, 154.48. EA: ($C_4H_4N_8O_3$, 212.1 g/mol) calcd: 22.65% C, 1.90% H, 52.82% N, found: 22.55% C, 2.3% H, 51.84% N; DSC (10 °C/min) T_{dec} at 352 °C. *IR* (cm^{-1}) ν = 3167.06, 3057.19, 2808.59, 1693.30, 1578.521534.32, 1442.86, 1133.50, 1013.81, 899.03, 810.03, 740. azotriazolone (azoTO) 1HNMR (600 MHz, DMSO-d_6, ppm) δ = 12.74 (s, 1H), 12.44 (s, 1H). ^{13}C NMR (150 Mz, DMSO-d_6, ppm) δ = 154.70, 154.76. EA: ($C_4H_4N_8O_2$, 196.1 g/mol) calcd: 24.50% C, 2.06% H, 57.13% N, found: 23.36% C, 2.16% H, 56.89%. *IR* (cm^{-1}) ν = 3142.5, 3054.7, 2950.9, 2831.3, 1682.8, 1540.4, 1468.6, 1426.9, 1286.9, 1118.8, 1040.8, 1018.1, 810.6, 745.6, 671.3, 482.9. BAM impact: > 40 J; BAM friction > 360 N.

3. Results and discussion

In order to understand the influence of sulfuric acid concentration on the yield of AZTO, NTO reduction experiments were carried out at different concentrations of sulfuric acid. Firstly, sulfuric acid with the concentration of 0.05 M, 0.1 M, 0.5 M, and 1 M H_2SO_4 was selected as the electrolyte, and the redox peaks of NTO (500 mg) at different concentrations were measured by cyclic voltammetry in this experiment. Fig. 1(a) shows the CV curve of NTO during electrolysis in H_2SO_4. It can be seen from Fig. 1(a) that, the reduction peaks of NTO shift to the direction of low potential as the increasing of electrolyte concentration, which indicates that NTO is more prone to secondary reduction and is not conducive to the synthesis of AZTO at high sulfuric acid concentration. In addition, the work quantitatively calculated the content of AZTO in the mixture of AZTO and azoTO by Hydrogen spectrum and obtained the relationship between the sulfuric acid concentration and the AZTO content. A mixture of AZTO and azoTO is obtained by washing the NTO electrolytic product. The total yield and AZTO percentage are listed in Table 1. It can be seen from Table 1 that as the electrolyte concentration decreases, the proportion and total yield of AZTO gradually increase. When the sulfuric acid concentration is 0.05 M, the proportion and total yield of AZTO reach the maximum, which are 67 % and 80 %, respectively. The above results indicate that the presence of acid may promote the further reduction reaction through proton-coupled electron transfer. Therefore, reducing the concentration of H_2SO_4 solution can inhibit the secondary reduction to some extent and improve the yield of AZTO {[26] #44}.

In the above analysis, we found that low-concentration sulfuric acid solution as the electrolyte is beneficial to the formation of AZTO. Therefore, Na_2SO_4 was selected as the electrolyte to explore the effect of a neutral electrolyte on the formation of AZTO. Fig. 1(b) is the CV curve of NTO electrolysis in Na_2SO_4 electrolyte. When the potential is -0.38 V, the two electrolytes have a reduction peak on the CV curve at the same position, which may be due to the same pH of the two solutions, which confirms the proton-coupled electron transfer effect. However, the other reduction peak was also observed at -0.83 V in the CV curve of 0.1 M Na_2SO_4. In the CV study of NTO, Na_2SO_4 was used as an electrolyte. From Fig. 1(b), it can be seen that both of them have a reduction peak at -0.38 V at the same time, which may be due to the same pH of the two solutions, which confirms the proton-coupled electron transfer effect. However, when 0.1 M Na_2SO_4 is used as the electrolyte, a second reduction peak appears at -0.83 V, which may be due to the fact that as the reaction proceeds, H^+ is continuously consumed. The AZTO synthesized by the electrochemical reduction of NTO exists in the form of anions, which promotes the solubility of AZTO in water, resulting in the secondary reduction of AZTO and the formation of a reduction peak. In the experiment of NTO electrolysis in Na_2SO_4 solution, the color of the electrolyte was observed to change gradually from yellow-green to orange-red, which indicated that the pH value of the electrolyte system changed from acidic to alkaline, and no precipitates were produced in

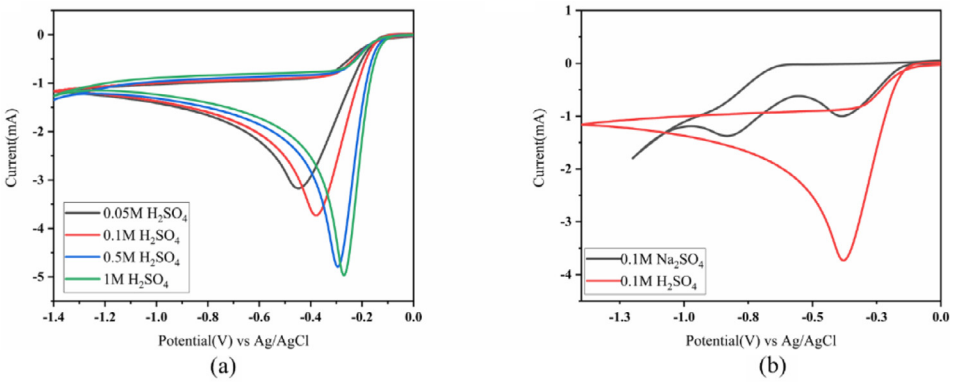

Fig. 1. (a) The CV of NTO in a 0.05 M, 0.1 M, 0.5 M, 1 M H_2SO_4 solution was accomplished using a 2 mm glassy carbon working electrode, a carbon plate counter electrode and an Ag/AgCl reference electrode at a rate of 0.1 V. (b) The CV of NTO in a 0.1 M H_2SO_4 and 0.1 M Na_2SO_4 solution was accomplished using a 2 mm glassy carbon working electrode, a carbon plate counter electrode and an Ag/AgCl reference electrode at a rate of 0.1 V.

Table 1
Results of the electrolysis of NTO using electrolytes with different sulphuric acid concentrations.

Entry	Temperature (°C)	Electrolyte	Electrodes	Potential (V)	Overall yield (%)	Proportion of AZTO (%)
1	5	0.05 M H_2SO_4	C/Pt	-1	67	88
2	5	0.1 M H_2SO_4	C/Pt	-1	63	80
3	5	0.5 M H_2SO_4	C/Pt	-1	55	64
4	5	1 M H_2SO_4	C/Pt	-1	50	56

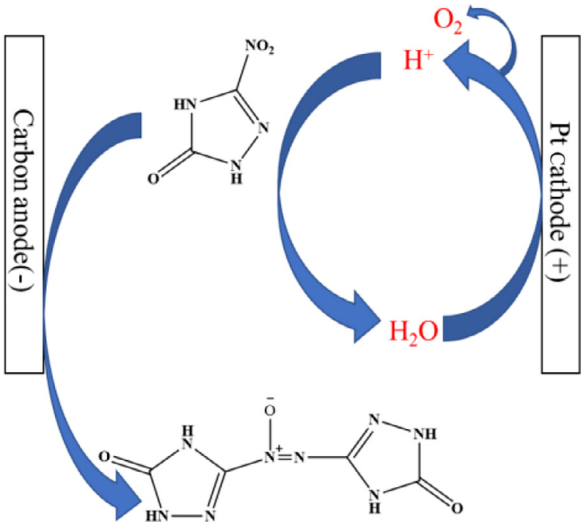

Fig. 2. A mechanism is proposed for the cathodic reduction of azo coupling of NTO to produce AZTO in acidic solutions.

the solution. However, a small amount of yellow precipitate was produced in the solution after acidification of the electrolyte with concentrated sulfuric acid, and the main component of that was identified by NMR hydrogen spectroscopy as azoTO. The experimental phenomena were consistent with the above analysis, which suggests the acidic electrolyte could avoid further reduction and increase the yield of AZTO by inhibiting the deprotonation of the triazole ring and reducing the solubility of AZTO in water. Based on the above results, the reaction mechanism of electrochemical reduction of NTO to AZTO is described in Fig. 2. By further optimizing the reaction conditions, it was found that the yield of AZTO could be further increased at low temperatures, and the experimental results were consistent with the literature reports. Attempts to further extend the electrolysis time found that part of AZTO was further reduced to azoTO, resulting in a decrease in the yield of AZTO.

3.1. Isolation and purification of AZTO and azoTO

AZTO and azoTO are insoluble in any solvent other than DMSO, such as methanol, ethanol, DMF, ethyl acetate, acetonitrile, etc. The solubility in water is also very low, so it cannot be separated and purified by column chromatography, and the DMSO/H_2O liquid phase diffusion crystallization will lead to an increase in the proportion of azoTO. Due to the deprotonation of the triazole ring, AZTO and azoTO can be miscible with water by increasing their solubility in water through salt-forming reactions with alkali. Therefore, we made the mixture of AZTO and azoTO completely dissolved in water by adding an excess of base, recrystallized it in water, and then redissolved the obtained solid in water and acidified by sulfuric acid, in order to obtain high-purity AZTO. However, it was found that AZTO and azoTO were not separated by ^{1}H NMR spectroscopy, and the proportion of azoTO was further increased. In view of this, this work uses the structural differences between AZTO and azoTO to find a method to separate them. For AZTO, the N-O bond in its structure can absorb electrons, which can further reduce the electron cloud density and promote the proton dissociation of the triazole ring. Theoretically, the acidity of AZTO is higher than that of azoTO, and it preferentially reacts with alkali to form salts. Therefore, it is only necessary to control the amount of alkali to make AZTO react completely, and through the difference in solubility between AZTO and azoTO to achieve separation and purification. To verify this conjecture, the mixture of AZTO and azoTO was dispersed in the appropriate amount of NaOH solution and stirred for 5 min to filter out the yellow precipitate. Then the pH of the filtrate was adjusted to 2 with concentrated sulfuric acid, and the yellow-green precipitate was obtained by filtration and drying. The two precipitates were tested by multinuclear NMR (^{1}H, ^{13}C). From Figs. 3 and 5, it can be seen that the ^{1}H NMR characteristic peaks of AZTO are 13.20 ppm, 12.48 ppm, 12.44 ppm and 12.08 ppm, and the ^{13}C NMR characteristic peaks are 144.85 ppm, 146.40 ppm, 154.10 ppm, 154.48 ppm, and no related peaks of azoTO are observed. From Figs. 4 and 6, it can be seen that the ^{1}H NMR characteristic peak of azoTO is 12.74 ppm, 12.44 ppm, and the ^{13}C NMR characteristic peak is 154.70 ppm, 154.76 ppm. The results show that, compared with azoTO, AZTO preferentially undergoes a salt-forming reaction with alkali. Taking advantage of this property, the separation and purification of AZTO and azoTO were successfully achieved.

Table 2
Results of electrolysis of NTO using different temperatures.

Entry	Temperature (°C)	Electrolyte	Electrodes	Potential (V)	Overall yield (%)	Proportion of AZTO (%)
1	5	0.1 M H_2SO_4	C/Pt	-1	63	80
2	10	0.1 M H_2SO_4	C/Pt	-1	58	72
3	20	0.1 M H_2SO_4	C/Pt	-1	48	55
4	30	0.1 M H_2SO_4	C/Pt	-1	42	43

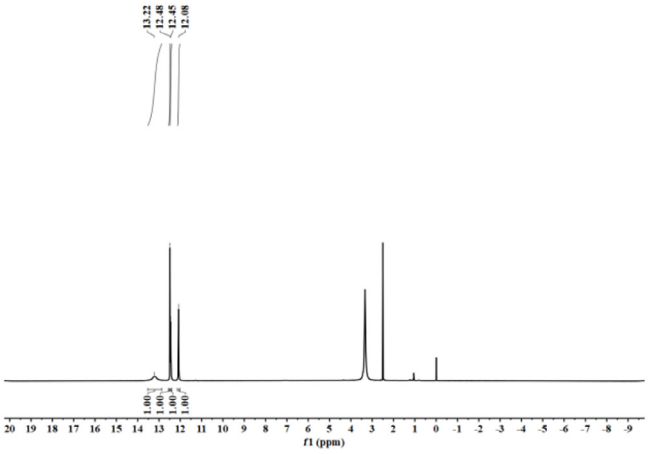

Fig. 3. ^{1}H NMR spectrum of AZTO.

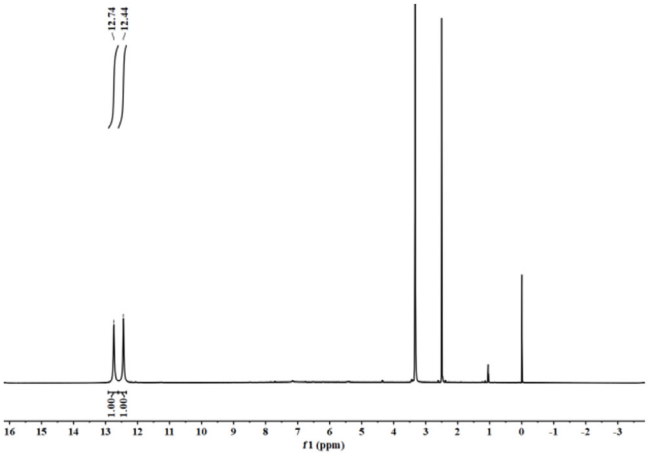

Fig. 4. ^{1}H NMR spectrum of azoTO.

3.2. Single crystal X-ray structure determinations

The AZTO crystal data and structural parameters are shown in Table 3, and the molecular structure diagram, hydrogen bond network diagram, and cell stacking diagram are shown in Figs. 7 and 8. The bond length information is listed in Table 4, the bond angle information is listed in Table 5, and the hydrogen bond information is listed in Table 6.

The crystal data for AZTO show that it belongs to the monoclinic system, $P2_1/n$ space group, with cell parameters of a = 6.5061(3) Å, b = 5.0081(3) Å, c = 11.4206(7) Å, α = 90°, β = 95.372°(2), γ = 90°, Z = 2 and a crystal density of 1.902 g/cm^3 measured at 193 K. From Fig. 5 it is clear that there is a disorder in the AZTO molecule and the O atom is found to be disordered, which is caused by the whole AZTO molecule being flipped by 180° {[27] #96}.

As displayed in Table 4, the bond length of N(2)-N(3) on the triazole ring is 1.363 Å, the N=N bond length connecting the triazole ring is 1.275 Å, both between the N-N single bond length (1.454 Å) and the N=N double bond length (1.245 Å), the N(4)-O(2) bond length is 1.222 Å, between the N-O bond length and the N=O double bond length, all C-N bond lengths and C=N bond lengths, are between the standard C-N (1.43 Å) and C=N (1.29 Å) bond lengths, and the C=O bond length is 1.2397 Å, between the standard C=O (1.21 Å) bond length and C-O (1.42

Table 3
Crystal data and structure refinement of AZTO

Compound	AZTO
CCDC	2183632
Empirical formula	$C_4H_4N_8O_3$
Formula weight	212.15
Temperature (K)	193.00
Crystal system	Monoclinic
Space group	P21/*n*
a (Å)	6.5061(3)
b (Å)	5.0081(3)
c (Å)	11.4206(7)
α (°)	90
β (°)	95.372(2)
γ (°)	90
Volume (Å^3)	370.49(4)
Z	2
P calc (g/cm^3)	1.902
F(000)	216.0
2Θ range for data collection (°)	6.942 to 54.958
Index ranges	$-8 \le h \le 7$, $-6 \le k \le 6$, $-13 \le l \le 14$
Goodness-of-fitonF^2	1.043
Final *R* indexes[I >= 2σ(I)]	*R*1 = 0.0427, *w*R2 = 0.1050
Final *R* indexes[all data]	*R*1 = 0.0472, *w*R2 = 0.1078

Table 4
Bond length of AZTO

Atoms1-2	*D*(1-2) (Å)	Atoms1-2	*D*(1-2) (Å)
O(1)-C(1)	1.2397(19)	N(4)-N(4)^1	1.275(3)
N(1)-C(1)	1.3736(18)	N(4)-C(2)	1.407(2)
N(1)-C(2)	1.362(2)	N(4)-O(2)	1.222(3)
N(2)-N(3)	1.363(2)	N(3)-C(2)	1.301(2)
N(2)-C(1)	1.353(2)		

Symmetric transformations for generating equivalent atoms:^{1}2-X,1-Y,1-Z

Table 5
Bond angles of AZTO

Atoms1–2–3	∢(1–2–3) (°)	Atoms1–2–3	∢(1–2–3) (°)
C(2)-N(1)-C(1)	106.27(13)	O(1)-C(1)-N(1)	127.53(15)
C(1)-N(2)-N(3)	113.26(13)	O(1)-C(1)-N(2)	128.35(14)
N(4)1-N(4)-C(2)	115.84(17)	N(2)-C(1)-N(1)	104.08(13)
O(2)-N(4)-N(4)1	130.3(2)	N(1)-C(2)-N(4)	127.12(14)
O(2)-N(4)-C(2)	113.45(18)	N(3)-C(2)-N(1)	113.42(14)
C(2)-N(3)-N(2)	102.97(14)	N(3)-C(2)-N(4)	119.45(15)

Symmetric transformations for generating equivalent atoms:^{1}2-X,1-Y,1-Z

Table 6
Hydrogen bond length and angle of AZTO

D-H…A	*d* (D-H) (Å)	*d* (H…A) (Å)	*d* (D…A) (Å)	∠DHA (°)
N(1)-H(1)…O(11)	0.88	2.01	2.8478(18)	159.6
N(2)-H(2)…O(12)	0.88	1.91	2.7819(18)	173.9

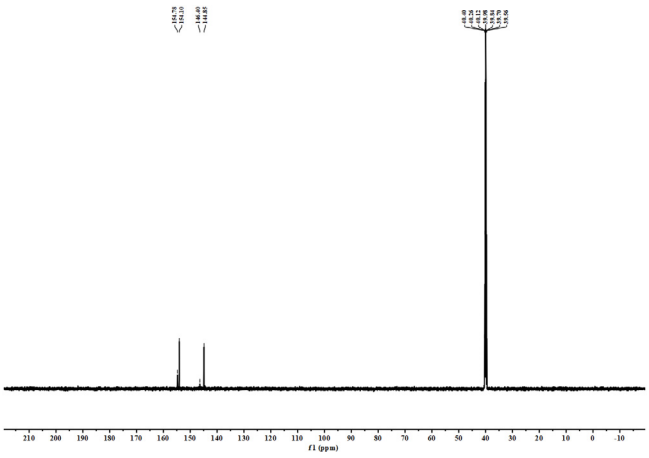

Fig. 5. ^{13}C NMR spectrum of AZTO.

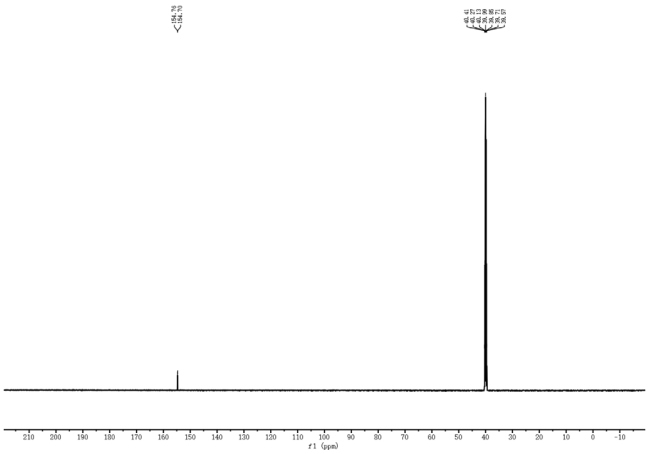

Fig. 6. ^{13}C NMR spectrum of azoTO.

Å) bond length, implying that the carbonyl oxygen atom is also involved in the conjugation. In summary, AZTO forms a larger conjugated system, which facilitates a lower electron cloud density.

From Fig. 8(a), it can be seen that the crystal stacking is dominated by a face-to-face Π-Π arrangement and the whole crystal shows a wave-like stacking; from Fig. 8(b) and Table 6, it can be seen that there are a large number of intermolecular hydrogen bonds between AZTO molecules. The crystal density and thermal stability of AZTO are improved due to the complex meshwork and Π-Π interactions formed by these hydrogen bonds.

3.3. Thermal stabilities

Thermal stability is an important indicator of whether energetic compounds can be applied to real life. The thermal stability of AZTO was investigated by thermogravimetric analysis and differential scanning calorimetric analysis (DSC/TGA). It was carried out at a heating rate of 10 K/min and under a nitrogen atmosphere. The DSC-TGA curves of AZTO and azoTO are shown in Fig. 9. AZTO and azoTO have good thermal stability. The decomposition temperatures of AZTO and azoTO are higher than 300 °C, better than NTO (273 °C) {[28] #97}. The thermal stability of high-purity AZTO(352 °C) is higher than that of low-purity AZTO (263 °C) {[20] #83}, indicating that the purity has a great influence on the thermal stability of AZTO. A small proportion of azoTO easily leads to the early decomposition of AZTO, so it is meaningful to find a suitable separation method.

3.4. Sensitivities properties

The impact sensitivity tests for AZTO and azoTO were carried out according to the modified instructions of the BFH PEx, using the Federal Bureau for Materials Research and Testing (BAM) falling hammer. Meanwhile, the friction sensitivity tests were executed on the BAM friction tester according to the modified instructions of FSKM10L, and the results were shown in Table 7. Table 7 depicts that the impact sensitivity of AZTO and azoTO is not less than 30 J and 40 J, and the friction sensitivity of those are greater than 360 N. AZTO is similar to NTO in impact sensitivity but higher than azoTO. In terms of friction sensitivity, AZTO and azoTO exhibit better stability than NTO.

3.5. Energetic properties

All independent variable calculations were carried out using the Gaussian09 package {[29] #88}. geometry optimisation and frequency calculations for the AZTO and azoTO structures were carried out using B3LYP/6-311G** and single-point energy calculations were carried out using MP2/6-311++G** {[30] #90}. The enthalpies of the formation of compounds are calculated from the isodesmic reactions. Based on the measured crystal densities and calculated enthalpies of generation, the detonation pressures (D) and detonation velocities (P) for AZTO and azoTO were calculated according to the Kamlet-Jacobs equations {[31] #91; [32] #92; [33] #94}, which are shown in Eqs. (1) and (2), and the results are shown in the Table 7.

$$D = 1.01\left(N\overline{M}^{0.5}Q^{0.5}\right)^{0.5}(1 + 1.30) \quad (1)$$

$$P = 1.558\rho^2\overline{M}^{0.5}Q^{0.5} \quad (2)$$

where each term in Eqs. (1) and (2) is defined as follows: D is the detonation velocity (m/s), P is the detonation pressure (GPa), and N is the moles of detonation gases per gram explosive, $\overline{M}$ is the average molecular mass of gaseous products (g/mol), Q and ρ are respectively the heat

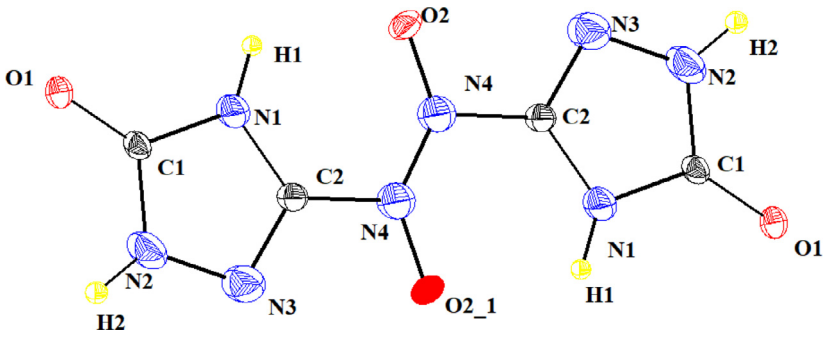

Fig. 7. Molecular structure of AZTO.

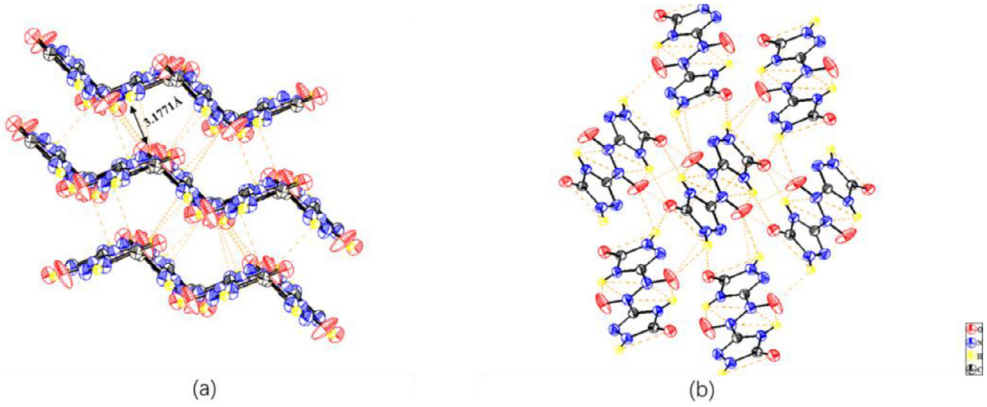

Fig. 8. (a) The crystal stacking of AZTO shows a planar conformation of the molecule as a result of Π-Π interactions with a planar spacing of 3.1771 Å. (b) Hydrogen bonding network diagram for AZTO.

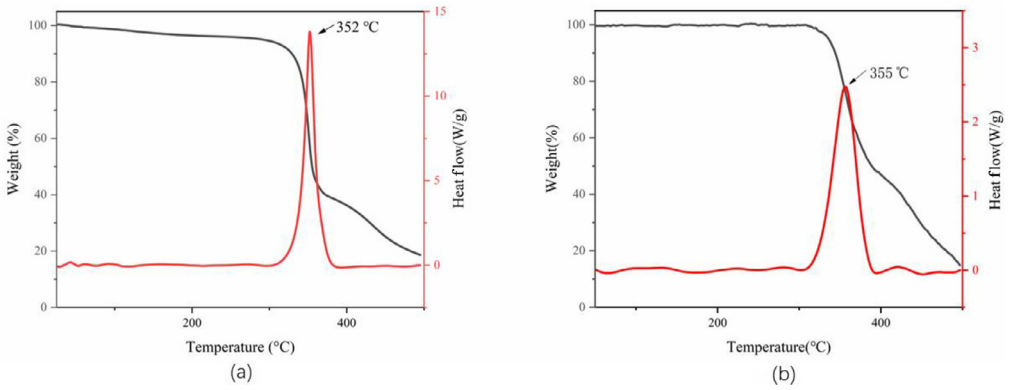

Fig. 9. (a)TGA and DSC curves of AZTO under nitrogen with a heating rate of 10 °C/min. (b) TGA and DSC curves of azoTO under nitrogen with a heating rate of 10 °C/min.

Table 7
Properties of energetic compounds

Compound	ρ[a] (g/cm^3)	N[b] (%)	T_{dec}[c] (°C)	Q[d] (kcal/g)	P[e] (GPa)	D[f] (m/s)	IS[g] (J)	FS[h] (N)
AZTO	1.902	55.98	352	0.653	26.1	7713.5	30	>360
azoTO	1.91[i]	51.84	355	0.880	23.8	7459.3	>40	>360
NTO[j]	1.91	43.1	273	0.983	33.4	8200	30	263
TNT	1.654	18.50	244	1.22	19.50	6881	15	353
RDX	1.80	37.80	210	1.44	33.92	8600	7	120

[a] From X-ray diffraction;
[b] Nitrogen content;
[c] Decomposition temperature (onset) under nitrogen (DSC, 10 °C/min);
[d] Heat of detonation;
[e] Detonation pressure;
[f] Detonation velocity;
[g] Impact sensitivity;
[h] Friction sensitivity;
[i] Ref. [20];
[j] Ref. [28].

of detonation (kcal/g) and the loaded density of explosives (g/cm^3). The measured single crystal density was used for the calculation here.

From Table 7, AZTO detonation speed of 7713.5 m/s, detonation pressure of 26.1 GPa, azoTO detonation speed of 7459.3 m/s, detonation pressure of 23.8 GPa, the detonation performance of both better than TNT (6881 m/s, 19.5 GPa). AZTO and azoTO show good thermal stability, both with thermal onset decomposition temperatures > 300 °C, and are more stable than RDX and TNT {[34] #95}.

4. Conclusions

In summary, this work successfully obtained a method for the separation and purification of AZTO and azoTO by using the difference in properties of AZTO and azoTO. The reaction conditions were further optimized and the related reaction mechanism was supplemented. In addition, AZTO Single crystal prepared by liquid-phase diffusion was tested to master the crystal structure. AZTO belongs to the monoclinic crystal system, with the space group of $P2_1/n$, and the crystal density at 193K is higher than that of other energetic materials, which is 1.902 g/cm^3. The results of TGA-DSC show that the high-purity AZTO obtained in this paper has good thermal stability (T_{dec} = 352 °C), which is related to the abundant hydrogen bonding and Π-Π interaction between its molecules. According to the enthalpy of formation and crystal density obtained from the experiment, the detonation parameters of AZTO and azoTO were calculated by the K-J empirical formula. The results illustrate that the detonation pressure and detonation velocity of AZTO (P = 26.1 GPa, D = 7713.5 m/s) and azoTO(P = 23.8 GPa, D = 7459.3 m/s) are superior to TNT (D = 6881 m/s, P = 19.5 GPa). And the impact sensitivity and friction sensitivity of AZTO (IS = 30 J, FS = 360 N) are also lower than those of the traditional energy-containing materials TNT

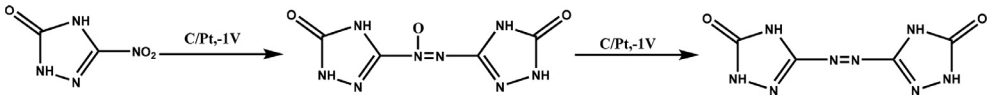

Scheme 1. Synthetic applications.

and RDX. The above analysis displays that the high-purity energetic material AZTO can be obtained by the scheme described in this paper, and AZTO has good performance (Scheme 1, Table 2).

Declaration of Competing Interests

The authors declare that they have no known competing financial interests or personal relationships that could have appeared to influence the work reported in this paper.

Acknowledgements

This research was supported by the project of State Key Laboratory of Environment-friendly Energy Material, Southwest University of Science and Technology (21fksy04).

References

[1] X. Peng, H. Chao, Chemistry with electrochemically generated N-Centered Radicals, Acc. Chem. Res. 52 (2019) 3339–3350.
[2] Y. Jiang, K. Xu, C. Zeng, Use of electrochemistry in the synthesis of heterocyclic structures, Chem. Rev. (2017) 7b00271 acs.chemrev.
[3] J. Gong, W. Luo, Y. Zhao, M. Xie, J. Wang, J. Yang, Y. Dai, Co_9S_8/$NiCo_2S_4$ core-shell array structure cathode hybridized with PPy/MnO2 core-shell structure anode for high-performance flexible quasi-solid-state alkaline aqueous batteries, Chem. Eng. J. 434 (2022) 134640.
[4] J. Gong, Y. Wang, J. Wang, Y. Liu, C. Hu, T. Zhou, Q. Yu, J. Yang, Y. Dai, Hollow nickel-cobalt sulfide nanospheres cathode hybridized with carbon spheres anode for ultrahigh energy density asymmetric supercapacitors, Int. J. Hydrogen Energy 47 (17) (2022) 10056–10068.
[5] J. Gong, J. Yang, J. Wang, L. Lv, W. Wang, L. Pu, H. Zhang, Y. Dai, A dual NiCo metal-organic frameworks derived $NiCo_2S_4$ core-shell nanorod arrays as high-performance electrodes for asymmetric supercapacitors, Electrochim. Acta 374 (2021) 137794.
[6] J. Gong, W. Luo, Y. Zhao, J. Wang, S. Wang, C. Hu, J. Yang, Y. Dai, Surface engineering of Ni wires and rapid growth strategy of Ni-MOF synergistically contribute to high-performance fiber-shaped aqueous battery, Small 18 (42) (2022) 2204346.
[7] W.L. Yuan, G.H. Tao, L. Zhang, Z. Zhang, W. Yu, Super impact stable TATB explosives recrystallized by bicarbonate ionic liquids with a record solubility, Sci. Rep. 10 (2020).
[8] M. Deng, Y. Feng, W. Zhang, X. Qi, Q. Zhang, A green metal-free fused-ring initiating substance, Nat. Commun. 10 (2019).
[9] V. Thottempudi, H. Gao, J.N.M. Shreeve, Trinitromethyl-substituted 5-nitro- or 3-azo-1,2,4-triazoles: synthesis, characterization, and energetic properties, J. Am. Chem. Soc. 133 (2011) 6464–6471.
[10] Z. Yan, T. Lu, Y. Liu, W. Liu, B. Zhao, Y. Wang, Z. Ge, 5,7-diamine-2-nitro-1,2,4-triazolo[1,5-a]-1,3,5-triazine (ANTT): a nitrogen-rich compound suitable for gas generators, FirePhysChem 2 (2022) 168–173.
[11] T.M. Klapötke, M. Leroux, P.C. Schmid, J. Stierstorfer, Energetic materials based on 5,5′-diamino-4,4′-dinitramino-3,3′-bi-1,2,4-triazole, Chem. Asian J. 11 (2016) 844–851.
[12] Edited by P. DerekH. Lund, O. Hammerich, M Dekker (Eds.), Organic Electrochemistry (2001) 1393. Edited by2001ISBN 0-8247-0430-4vii +US$275.00Journal of Electroanalytical Chemistry.
[13] E.J. Horn, B.R. Rosen, P.S. Baran, Synthetic organic electrochemistry: an enabling and innately sustainable method, ACS Cent. Sci. (2016) 6b00091 acscentsci.
[14] Y. Yuan, A. Lei, Is electrosynthesis always green and advantageous compared to traditional methods? Nat. Commun. 11 (2020) 802.
[15] L. Chen, L.M. Barton, J.C. Vantourout, Y. Xu, C. Chu, E.C. Johnson, J.J. Sabatini, P.S. Baran, Electrochemical cyclobutane synthesis in flow: scale-up of a promising melt-castable energetic intermediate, Org. Process Res. Dev. 25 (2020) 2639–2645.
[16] H. He, J. Du, B. Wu, X. Duan, Y. Zhou, G. Ke, T. Huo, Q. Ren, L. Bian, F. Dong, Photoelectrochemical driving and clean synthesis of energetic salts of 5,5′-azotetrazolate at room temperature, Green Chem. 20 (2018) 3722–3726.
[17] S.C. Chew, M. Tennant, N. Mai, D. McAteer, J.F. Pons, Practical remediation of 3-nitro-1,2,4-triazol-5-one wastewater, Propellants Explos. Pyrotech. 43 (2017) 198–202.
[18] C.L. Madeira, J.A. Field, M.T. Simonich, R.L. Tanguay, J. Chorover, R. Sierra-Alvarez, Ecotoxicity of the insensitive munitions compound 3-nitro-1,2,4-triazol-5-one (NTO) and its reduced metabolite 3-amino-1,2,4-triazol-5-one (ATO), J. Hazard. Mater. 343 (2018) 340–346.
[19] M.P. Cronin, A.I. Day, L. Wallace, Electrochemical remediation produces a new high--nitrogen compound from NTO wastewaters, J. Hazard. Mater. 149 (2007) 527–531.
[20] C.J. Underwood, C. Wall, A. Provatas, L. Wallace, New high nitrogen compounds azoxytriazolone (AZTO) and azotriazolone (azoTO) as insensitive energetic materials, New J. Chem. 36 (2012) 2613.
[21] O.V. Dolomanov, L.J. Bourhis, R.J. Gildea, J.A.K. Howard, H. Puschmann, OLEX2: a complete structure solution, refinement and analysis program, J. Appl. Crystallogr. 42 (2009) 339–341.
[22] G.M. Sheldrick, SHELXT – integrated space-group and crystal-structure determination, Acta Crystallogr. A Found. Adv. 71 (2015) 3–8.
[23] G.M. Sheldrick, A short history of SHELX, Acta Crystallogr. A 64 (2007) 112–122.
[24] R.R. Sirach, P.N. Dave, 3-nitro-1,2,4-triazol-5-one (NTO): high explosive insensitive energetic material, Chem. Heterocycl. Compd. 57 (2021) 720–730.
[25] L. Wallace, C.J. Underwood, A.I. Day, D.P. Buck, Electrochemical reduction of nitrotriazoles in aqueous media as an approach to the synthesis of new green energetic materials, New J. Chem. 35 (2011) 2894.
[26] J.R. Yount, M. Zeller, E.F.C. Byrd, D.G. Piercey, 4,4′,5,5′-Tetraamino-3,3′-azo-bis-1,2,4-triazole and the electrosynthesis of high-performing insensitive energetic materials, J. Mater. Chem. A 8 (2020) 19337–19347.
[27] E.Y. Cheung, L.D. Pennington, M.D. Bartberger, R.J. Staples, 2,2′-Bi[benzo[b]thiophene]: an unexpected isolation of the benzo[b]thiophene dimer, Acta Crystallogr. C Struct. Chem. 70 (2014) 547–549.
[28] P. Pagoria, A comparison of the structure, synthesis, and properties of insensitive energetic compounds, Propellants Explos. Pyrotech. 41 (2016) 452–469.
[29] M.e. Frisch, G. Trucks, H. Schlegel, G. Scuseria, M. Robb, J. Cheeseman, G. Scalmani, V. Barone, G. Petersson, H. Nakatsuji, Gaussian 16, Gaussian, Inc, Wallingford, CT, 2016.
[30] B.M. Rice, J.J. Hare, E. Byrd, Accurate predictions of crystal densities using quantum mechanical molecular volumes, J. Phys. Chem. A 111 (2007) 10874–10879.
[31] M.J. Kamlet, S.J. Jacobs, Chemistry of detonations. I. A simple method for calculating detonation properties of C–H–N–O explosives, J. Chem. Phys. 48 (1968) 23–35.
[32] F. Bao, G. Zhang, S. Jin, Y. Zhang, Q. Shu, L. Li, Theoretical study of the heats of formation, detonation properties, and bond dissociation energies of substituted bis-1,2,4-triazole compounds, J. Mol. Model. 24 (2018) 85.
[33] P. Politzer, J.S. Murray, Some perspectives on estimating detonation properties of C, H, N, O compounds, Cent. Eur. J. Energetic Mater. 8 (2011) 209–220.
[34] Y. Zhang, S. Zhang, L. Sun, Q. Yang, J. Han, Q. Wei, G. Xie, S. Chen, S. Gao, A solvent-free dense energetic metal-organic framework (EMOF): to improve stability and energetic performance via in situ microcalorimetry, Chem. Commun. (Camb.) 53 (2017) 3034–3037.